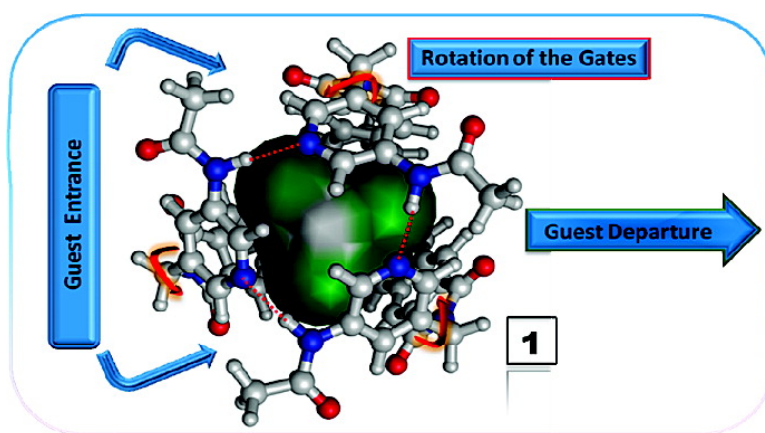


## A 3-fold “Butterfly Valve” in Command of the Encapsulation’s Kinetic Stability. Molecular Baskets at Work

Bao-Yu Wang, Xiaoguang Bao, Zhiqing Yan, Veselin Maslak, Christopher M. Hadad, and Jovica D. Badjic#

*J. Am. Chem. Soc.*, **2008**, 130 (45), 15127-15133 • DOI: 10.1021/ja8041977 • Publication Date (Web): 21 October 2008

Downloaded from <http://pubs.acs.org> on February 8, 2009



### More About This Article

Additional resources and features associated with this article are available within the HTML version:

- Supporting Information
- Links to the 1 articles that cite this article, as of the time of this article download
- Access to high resolution figures
- Links to articles and content related to this article
- Copyright permission to reproduce figures and/or text from this article

[View the Full Text HTML](#)

## A 3-fold “Butterfly Valve” in Command of the Encapsulation’s Kinetic Stability. Molecular Baskets at Work

Bao-Yu Wang, Xiaoguang Bao, Zhiqing Yan, Veselin Maslak,  
Christopher M. Hadad, and Jovica D. Badjić\*

Department of Chemistry, The Ohio State University, 100 West 18th Avenue,  
Columbus, Ohio 43210

Received June 10, 2008; E-mail: badjic@chemistry.ohio-state.edu

**Abstract:** Molecular basket **1**, composed of a semirigid *tris*-norbornadiene framework and three revolving pyridine-based gates at the rim, has been built to “dynamically” enclose space and as such regulate molecular encapsulation. The gates were shown to fold via intramolecular hydrogen bonding and thereby form a  $C_{3v}$  symmetrical receptor: the  $^1\text{H}$  NMR resonance for the amide N–H protons of the pyridine gates appeared downfield ( $\delta = 10.98$  ppm), and the N–H vibrational stretch (IR) was observed at  $3176\text{ cm}^{-1}$ . Accordingly, density functional theory (DFT, B3LYP) investigations revealed for the closed conformers of **1** to be energetically the most stable and dominant. The gearing of the pyridine “gates”, about their axis, led to the interconversion of two dynamic enantiomers **1**<sub>A</sub> and **1**<sub>B</sub> comprising the clockwise and counterclockwise seam of intramolecular hydrogen bonds. Dynamic  $^1\text{H}$  NMR spectroscopic measurements and line-shape simulations suggested that the energy barrier of  $10.0\text{ kcal/mol}$  ( $\Delta G_{A/B}^\ddagger$ , 298 K) is required for the **1**<sub>A/B</sub> interconversion, when  $\text{CCl}_4$  occupies the cavity of **1**. Likewise, the activation free energy for  $\text{CCl}_4$  departing the basket was found to be  $13.1\text{ kcal/mol}$  ( $\Delta G^\ddagger$ , 298 K), whereas the thermodynamic stability of **1**: $\text{CCl}_4$  complex was  $-2.7\text{ kcal/mol}$  ( $\Delta G^\circ$ , 298 K). In view of that,  $\text{CCl}_4$  (but also  $(\text{CH}_3)_3\text{CBr}$ ) was proposed to escape from, and a molecule of solvent to enter, the basket when the gates rotate about their axis: the exit of  $\text{CCl}_4$  requires the activation energy of  $12.7\text{ kcal/mol}$  ( $\Delta G_{A/B}^\ddagger + \Delta G^\circ$ ), similar to the experimentally found  $13.1\text{ kcal/mol}$  ( $\Delta G^\ddagger$ ).

### Introduction

The molecular trafficking in natural systems is governed via programmed and dynamic chemical processes.<sup>1</sup> Complex operations, such as selective transport of molecules<sup>2</sup> and catalysis,<sup>3</sup> are thus repeatedly executed in a precise manner, albeit challenging to duplicate into functional artificial systems.<sup>4</sup> Acetylcholinesterase, for instance, regulates its specificity without sacrificing efficiency through a mechanism of conformation gating:<sup>5</sup> stochastically controlled entry, inside a deep gorge leading to the enzyme active site, opens for a small fraction of time to modulate the guest’s incoming rate as a

function of its size. The substrate binding rate for smaller guests ( $<2.4\text{ \AA}$  radius), thereby, becomes modestly reduced, whereas bulkier substrates ( $>2.8\text{ \AA}$  radius) experience a considerable decrease in the rate of access to the active site; the fluctuating constriction of the entrance brings a required selectivity without sacrificing the catalytic efficiency! In unnatural systems,<sup>6</sup> however, conformationally dynamic groups at the skin of hemicarcerands<sup>7</sup> have afforded a measurable gain in kinetic stability of the complexes via gating access to the host’s interior. Notably, investigating novel ways for directing molecular encapsulation<sup>8</sup> and constrictive binding<sup>9</sup> will provide insight into understanding the molecular translocation in unnatural environ-

- (1) *Essays in Biochemistry: Molecular Trafficking*; Bernstein, P., Ed.; Portland Press: London, 2000.
- (2) Pallotta, B. S. *Ann. N.Y. Acad. Sci.* **1997**, *812*, 133–140.
- (3) Swift, R. V.; McCammon, J. A. *Biochemistry* **2008**, *47*, 4102–4111.
- (4) For selected references, see: (a) Badjić, J. D.; Ronconi, C. M.; Stoddart, J. F.; Balzani, V.; Silvi, S.; Credi, A. *J. Am. Chem. Soc.* **2006**, *128*, 1489–1499. (b) Pei, R.; Taylor, S. K.; Stefanovic, D.; Rudchenko, S.; Mitchell, T. E.; Stojanovic, M. N. *J. Am. Chem. Soc.* **2006**, *128*, 12693–12699. (c) Wintjes, N.; Bonifazi, D.; Cheng, F.; Kiebele, A.; Stoehr, M.; Jung, T.; Spillmann, H.; Diederich, F. *Angew. Chem., Int. Ed.* **2007**, *46*, 4089–4092. (d) Hidalgo, R. P.; Coumans, R. G. E.; Deutman, A. B. C.; Smits, J. M. M.; De Gelder, R.; Elemans, J. A. A. W.; Nolte, R. J. M.; Rowan, A. E. *J. Am. Chem. Soc.* **2007**, *129*, 5699–5702. (e) Percec, V.; Rudick, J. G.; Peterca, M.; Heiney, P. A. *J. Am. Chem. Soc.* **2008**, *130*, 7503–7508. (f) Angelos, S.; Yang, Y.-W.; Patel, K.; Stoddart, J. F.; Zink, J. I. *Angew. Chem., Int. Ed.* **2008**, *47*, 2222–2226. (g) Stock, C.; Heureux, N.; Browne, W. R.; Feringa, B. L. *Chem.-Eur. J.* **2008**, *14*, 3146–3153.
- (5) Zhou, H.-X.; Wlodek, S. T.; McCammon, J. A. *Proc. Natl. Acad. Sci. U.S.A.* **1998**, *95*, 9280–9283.

- (6) (a) Talukdar, P.; Bollot, G.; Mareda, J.; Sakai, N.; Matile, S. *Chem.-Eur. J.* **2005**, *11*, 6525–6532. (b) Gokel, G. W.; Leevy, W. M.; Weber, M. E. *Macrocycl. Chem.* **2005**, 253–265.
- (7) (a) Houk, K. N.; Nakamura, K.; Sheu, C.; Keating, A. E. *Science* **1996**, *273*, 627–629. (b) Sheu, C.; Houk, K. N. *J. Am. Chem. Soc.* **1996**, *118*, 8056–8070.
- (8) For selected examples, see: (a) Rudkevich, D. M.; Hilmersson, G.; Rebek, J., Jr. *J. Am. Chem. Soc.* **1998**, *120*, 12216–12225. (b) Vysotsky, M. O.; Thondorf, I.; Bohmer, V. *Angew. Chem., Int. Ed.* **2000**, *39*, 1264–1267. (c) Zuccaccia, D.; Pirondini, L.; Pinalli, R.; Jaun, B.; Diederich, F. *Angew. Chem., Int. Ed.* **2005**, *44*, 7025–7032. (d) Hooley, R. J.; Anda, H. J. V.; Rebek, J., Jr. *J. Am. Chem. Soc.* **2006**, *128*, 3894–3895. (e) Mukhopadhyay, P.; Zavalij, P. Y.; Isaacs, L. J. *J. Am. Chem. Soc.* **2006**, *128*, 14093–14102. (f) Gottschalk, T.; Jaun, B.; Diederich, F. *Angew. Chem., Int. Ed.* **2007**, *46*, 260–264. (g) Pluth, M. D.; Bergman, R. G.; Raymond, K. N. *Angew. Chem., Int. Ed.* **2007**, *46*, 8587–8589.
- (9) Liu, Y.; Warmuth, R. *Org. Lett.* **2007**, *9*, 2883–2886.

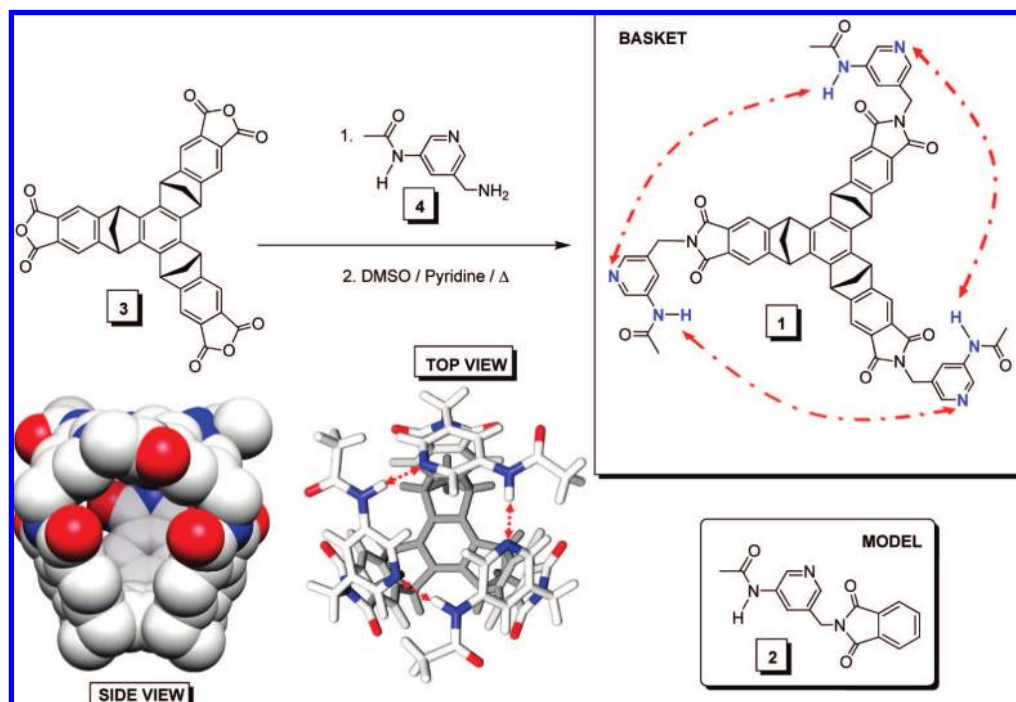


**Figure 1.** Chemical structures and synthesis of molecular basket **1** and model compound **2**. Top and side views of energy-minimized (DFT, B3LYP) structure of folded **1**.

ments. Furthermore, these endeavors will facilitate the rational design of newly formulated catalysts and molecular devices.<sup>10</sup>

In that vein, the present study has been directed toward developing a functional and modular abiotic receptor, molecular basket, for regulating the kinetics ( $k_{\text{on/off}}$ ) of molecular encapsulation. The ambiguity of synchronizing the host dynamics with the course of the guest exchange<sup>11</sup> has been addressed in this study by developing an approach so that one can learn about controlling the gating of molecules in artificial systems. Molecular baskets (Figure 1) were originally made<sup>12</sup> to incorporate a concave-shaped  $C_{3v}$  symmetrical tris-norbornadiene framework. Three aromatic rings, containing transition-metal chelating<sup>13</sup> or hydrogen-bonding<sup>12a</sup> sites, have been installed at the rim to act as “gates” in: (a) controlling the basket’s folding, (b) the formation of its “dynamic” interior, and (c) the in/out trafficking of the guest(s). The conformational dynamics of the hydrogen-bonded host<sup>12a</sup> was, in particular, revealed to have an adverse effect on the thermodynamics of the guest encapsulation. A notion that more “restricted” gates that hold to each other at two “points” could be incorporated in the basket’s design was exercised in constructing compound **1** (Figure 1).

This receptor was therefore envisaged to contain three pyridine gates, each with an acetylated amide unit, predisposed to form intramolecular hydrogen bonds (HBs) and thereby physically enfold space (Figure 1). In particular, learning about the relationship between the folding characteristics of the basket, its conformational dynamics (opening/closing), and the guest exchange was of great interest. The present study, for the first time, reveals such a dependence and, concomitantly, offers these dynamic receptors as convenient models for investigating the fundamentals of molecular trafficking.

## Results and Discussion

**Synthesis.** Molecular basket **1** was obtained (63% yield) by condensation of tris-anhydride **3** with acetylated (aminomethyl)pyridine **4** (Figure 1). The reaction was completed in dimethyl sulfoxide, when promoted with a catalytic amount of pyridine. Likewise, model compound **2** was synthesized from phthalic anhydride (Figure 1).

**<sup>1</sup>H NMR Spectroscopic Studies – Intramolecular versus Intermolecular Contacts.** The <sup>1</sup>H NMR spectrum (400 MHz, 298 K) of **1** in CDCl<sub>3</sub> has been assigned to a  $C_3$  symmetrical molecule (Figure 2B). The signal for the N–H proton appeared downfield ( $\delta = 10.98$  ppm) and stayed constant as the CDCl<sub>3</sub> solution was diluted from 20 to 0.5 mM. Respectively, the <sup>1</sup>H NMR resonance for the N–H proton in model compound **2** was found at a higher field ( $\delta = 7.30$  ppm, Figure 2A). The resonance underwent an upfield shift ( $\Delta\delta = 0.3$  ppm) with solvent dilution from 13.0 to 0.1 mM. The spectroscopic results, unequivocally, support the occurrence of stable intramolecular HBs in **1**. The observed <sup>1</sup>H NMR responsiveness of the N–H resonance in model **2** with the dilution is, however, in agreement with this compound’s propensity toward forming intermolecular HBs. Furthermore, the temperature-dependent <sup>1</sup>H NMR chemical shift coefficient,  $\Delta\delta/\Delta T$ , for the N–H resonance in **1**, was

- (10) (a) Davis, A. V.; Yeh, R. M.; Raymond, K. N. *Proc. Natl. Acad. Sci. U.S.A.* **2002**, *99*, 4793–4796. (b) Vriezema, D. M.; Aragonés, M. C.; Elemans, J. A. A. W.; Cornelissen, J. J. L. M.; Rowan, A. E.; Nolte, R. J. M. *Chem. Rev.* **2005**, *105*, 1445–1489. (c) Yoshizawa, M.; Tamura, M.; Fujita, M. *Science* **2006**, *312*, 251–254. (d) Yu, J.; RajanBabu, T. V.; Parquette, J. R. *J. Am. Chem. Soc.* **2008**, *130*, 7845–7847.
- (11) See, for instance: Palmer, L. C.; Rebek, J., Jr. *Org. Biomol. Chem.* **2004**, *2*, 3051–3059.
- (12) (a) Maslak, V.; Yan, Z.; Xia, S.; Gallucci, J.; Hadad, C. M.; Badjić, J. D. *J. Am. Chem. Soc.* **2006**, *128*, 5887–5894. (b) Yan, Z.; McCracken, T.; Xia, S.; Maslak, V.; Gallucci, J.; Hadad, C. M.; Badjić, J. D. *J. Org. Chem.* **2008**, *73*, 355–363.
- (13) (a) Yan, Z.; Xia, S.; Gardlik, M.; Seo, W.; Maslak, V.; Gallucci, J.; Hadad, C. M.; Badjić, J. D. *Org. Lett.* **2007**, *9*, 2301–2304. (b) Rieth, S.; Yan, Z.; Xia, S.; Gardlik, M.; Chow, A.; Fraenkel, G.; Hadad, C. M.; Badjić, J. D. *J. Org. Chem.* **2008**, *73*, 5100–5109.

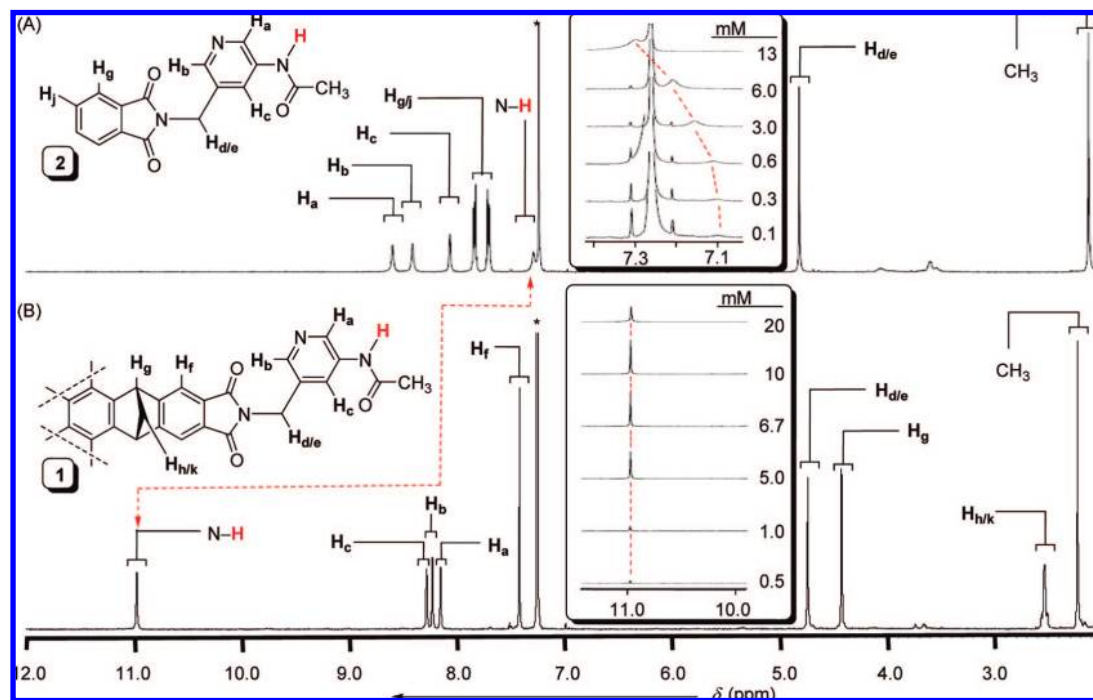


**Figure 2.**  $^1\text{H}$  NMR spectra (400 MHz, 298 K) of (A) model compound **2** (13.0 mM) and (B) molecular basket **1** (1.87 mM) in  $\text{CDCl}_3$ . Insets: segments of  $^1\text{H}$  NMR spectra showing the N–H resonance shift of **2** (top) and **1** (bottom), recorded in dilution experiments.

found to be 6.1 ppb/K (298 to 197 K).<sup>14</sup> The low value is in agreement with the absence of complex equilibria and the N–H protons residing in alternative environments at variable temperatures. Molecular basket **1** was also shown to stay predominantly monomeric and incapable of intermolecular aggregation in solution.  $^1\text{H}$  NMR DOSY measurements (500 MHz, 298 K,  $\text{CDCl}_3$ ) of **1** revealed that the apparent diffusion coefficients  $D^{\text{app}}$  are practically invariant ( $5.6$  and  $5.9 \times 10^{-10} \text{ m}^2 \text{ s}^{-1}$ ) at concentrations of 13.0 and 0.7 mM, respectively.<sup>14</sup> Additionally, MALDI mass spectrometry measurements of **1** revealed only the monomeric form.<sup>14</sup>

**Conformational Studies: Infrared Spectroscopy and Theoretical Calculations.** The design algorithm incorporated in the structure of **1** was to allow for the exclusive formation of a seam of intramolecular N–H...N HBs (Figure 1) on the rim of the basket. The desired outcome required additional scrutiny of the observed  $^1\text{H}$  NMR spectra, illustrating the intramolecular interactions of **1** in detail. The FT-IR spectrum of model compound **2** revealed a sharp band at  $3431 \text{ cm}^{-1}$  ( $\text{CHCl}_3$ ), corresponding to the N–H stretching vibration that is free of intermolecular interactions.<sup>14</sup> Molecular basket **1** ( $\text{CDCl}_3$ ), however, showed the corresponding vibration<sup>14</sup> as a concentration-independent (20.0 to 1.0 mM) broadband at  $3176 \text{ cm}^{-1}$ , in good agreement with strong intramolecular HBs. In the same region of the IR spectrum of **1** ( $3100\text{--}3150 \text{ cm}^{-1}$ ), however, there were apparent satellite signals<sup>14</sup> suggesting a potential conformational distribution.

Secondary amides, such as **1**, can exhibit *E/Z* isomerization,<sup>15</sup> leading to different intramolecular HB patterns. Energy minimizations (density functional theory, B3LYP)<sup>16</sup> of **1** demonstrated the folded [*Z*<sup>3</sup>] isomer as thermodynamically the most

**Table 1.** Computed Relative Thermodynamic Parameters (DFT, B3LYP) for the Stereoisomers of **1** (kcal/mol), and Their Boltzmann Distribution (Population) in the Gas Phase (298 K)

molecular basket <b>1</b>	B3LYP/6-31G(d) <sup>a</sup>		B3LYP/6-311+G(d,p) <sup>a</sup>		population (%)
	$\Delta H^\circ$	$\Delta G^{\circ b}$	$\Delta H^\circ$	$\Delta G^{\circ b}$	
[ <i>Z</i> <sup>3</sup> ]	0	0	0	0	97
[ <i>Z</i> <sup>2</sup> <i>E</i> ]	3.56	3.41	4.03	3.92	1
[ <i>ZE</i> <sup>2</sup> ]	6.61	7.57	7.51	8.45	0
[ <i>E</i> <sup>3</sup> ]	9.10	11.52	10.54	12.96	0
[ <i>Z</i> <sup>3</sup> –HB]	3.97	2.64	3.97	2.65	2

<sup>a</sup> In kcal/mol, using the optimized B3LYP/6-31G(d) geometry.

<sup>b</sup> Corrected for the statistical degeneracy.

stable (Table 1), with other structures ([*Z*<sup>2</sup>*E*], [*ZE*<sup>2</sup>], [*E*<sup>3</sup>]) populating the equilibrium to a much lesser degree (Table 1).<sup>14</sup> Importantly, further theoretical studies revealed the existence of a conformer of **1** (Figure 1), lacking one hydrogen bond ([*Z*<sup>3</sup>–HB]), Table 1,<sup>14</sup> and this conformer was computed to populate the equilibrium to about 2% (Table 1). The IR result can thus be qualitatively put in agreement with the basket being folded via the engineered N–H...N seam of hydrogen bonds (Figure 1) at the rim of the basket, albeit with a population distribution indicating an existence of other isomeric structures.<sup>17</sup>

**Conformational Stereoisomerism: 2D and Dynamic  $^1\text{H}$  NMR Spectroscopic Measurements.** The results of two-dimensional  $^1\text{H}$ – $^1\text{H}$  ROESY spectroscopic measurements of **1** gave further support to the projected folding pattern and indicated the existence of a dynamic equilibrium **1**<sub>A</sub>/**1**<sub>B</sub> (Figure 3).<sup>14</sup> The magnetization transfer (ROE) through space was detected for **H**<sub>a</sub>, but not **H**<sub>c</sub>, and N–H resonances of the gates (Figure 3A). The result indicated a restricted rotation of the

(14) See Supporting Information for more details.

(15) Ilieva, S.; Hadjieva, B.; Galabov, B. *J. Mol. Spectrosc.* **1999**, *508*, 73–80.

(16) (a) Perdew, J. P. *Phys. Rev. B* **1986**, *33*, 8822. (b) Becke, A. D. *Phys. Rev. A* **1998**, *38*, 3098.

(17) Presently, we are investigating the conformational characteristics of **1** using various theoretical models for the solvation. These procedures will afford a more “realistic” conformational energy landscape and, perhaps, allow us to reproduce the experimentally observed infrared spectra.

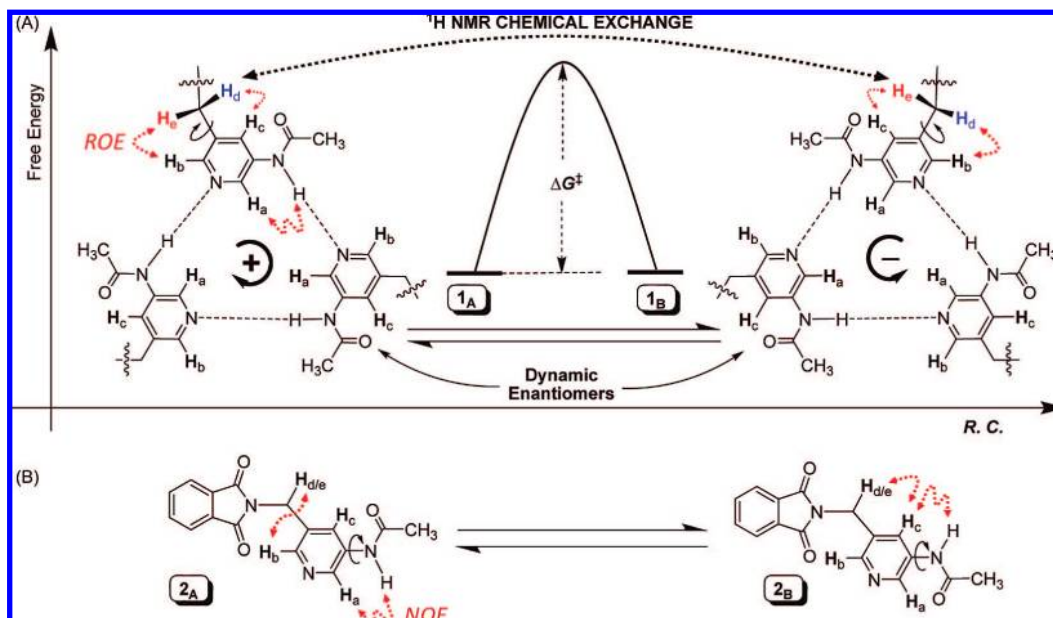


**Figure 3.** (A) Clockwise and counterclockwise arrangements of the seam of hydrogen bonds in dynamic enantiomers **1<sub>A</sub>** and **1<sub>B</sub>**, respectively. (B) Two conformers of **2** obtained by 180° rotation of the appended amide about the Ar–NH  $\sigma$  bond. The observed ROE and NOE signals in **1** and **2** (CDCl<sub>3</sub>, 400 MHz, 300 K), respectively, are shown in red.

appended amide(s) about the Ar–NH bond(s) and is a corollary of the constraint imposed by the seam of the intramolecular N–H...N HBs in **1** (Figure 3A). On the contrary, model compound **2** cannot engage in such intramolecular interactions, and the rotation about its Ar–NH bond was indeed found to be unhindered: the NOE cross peaks were detected for both **H<sub>d/e</sub>** and the N–H (Figure 3B)!

The projected seam of HBs in **1** is dynamic and displayed in either clockwise (+, **1<sub>A</sub>**) or counterclockwise (–, **1<sub>B</sub>**) direction of the N–H...N connections (Figure 3A). The gearing of the pyridine “gates”, about their axis, should thus permit the interconversion of the dynamic enantiomers **1<sub>A</sub>** and **1<sub>B</sub>**. This effect, as monitored by <sup>1</sup>H NMR spectroscopy, would lead to the chemical exchange of the “hinge” **H<sub>d/e</sub>** protons; the exchange process would distinguish these protons as being diastereotopic at low and enantiotopic at high temperatures. Indeed, the dynamic <sup>1</sup>H NMR studies of **1** revealed the **H<sub>d/e</sub>** resonance(s) appear as a four-line AB-type quartet at low and a singlet at high temperatures (Figure 4), verifying the **1<sub>A/B</sub>** equilibrium!

**The Inner Phase Solvation and the Host’s Dynamics.** Interestingly, the **H<sub>d/e</sub>** signal decoalescence was observed in CDCl<sub>3</sub> at a higher temperature (~225 K), while in CD<sub>2</sub>Cl<sub>2</sub> at a considerably lower temperature (<183 K).<sup>14</sup> At first, this came as a surprise because the conformational **1<sub>A/B</sub>** interconversion must entail the rupture of the intramolecular HBs, for which the stability should be almost invariant in these two, noncoordinating and low-polarity, solvents.<sup>18</sup> Accordingly, a perception that more sizable CHCl<sub>3</sub> (75 Å<sup>3</sup>) fits better inside of **1** (~221 Å<sup>3</sup>)<sup>14</sup> than smaller CD<sub>2</sub>Cl<sub>2</sub> (61 Å<sup>3</sup>) arose. In fact, the computational studies (PM3, CAChe) suggested that the egress of CH<sub>2</sub>Cl<sub>2</sub>, along a reaction coordinate directed through the center of an aperture of the folded host,<sup>7</sup> necessitates a lower activation energy (~7 kcal/mol) than the expulsion of CHCl<sub>3</sub> (~14 kcal/mol).<sup>14</sup> Dichloromethane was, for that reason, concluded to be

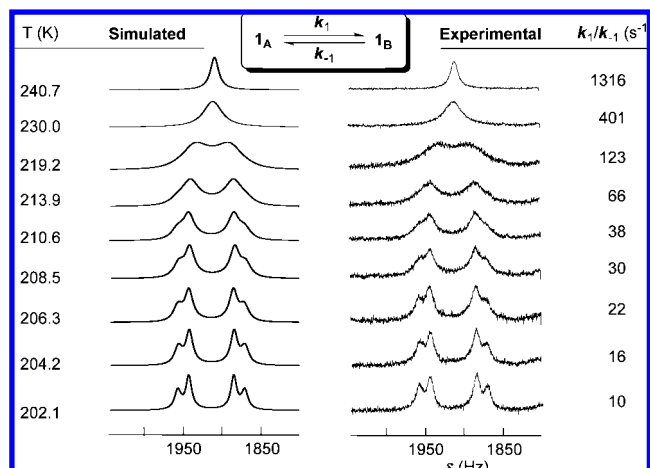


**Figure 4.** Simulated and experimental (WINDNMR-Pro)<sup>23</sup> resonances for the **H<sub>d/e</sub>** protons in **1** (CDCl<sub>3</sub>, 1.17 mM). Apparent first-order rate constants  $k_1/k_{-1}$  for the **1<sub>A</sub>/1<sub>B</sub>** interconversion at the examined temperatures.

less competitive for occupying the inner space of the basket,<sup>9</sup> and hence more suitable for investigating its host-like behavior!<sup>19</sup>

**Recognition Studies: The Thermodynamics of CCl<sub>4</sub> and CHCl<sub>3</sub> Entrapment.** A gradual addition of CCl<sub>4</sub> to a solution of **1** (2.98 mM) in CD<sub>2</sub>Cl<sub>2</sub> caused considerable changes in its <sup>1</sup>H NMR spectrum.<sup>14</sup> The N–H resonance shifted to a lower field ( $\Delta\delta = 0.5$  ppm), as the concentration of CCl<sub>4</sub> was gradually increased. The nonlinear curve fitting of the binding isotherm,<sup>20</sup> to a 1:1 stoichiometric model, yielded an apparent association constant of  $K_a^{298} = 109 \pm 1$  M<sup>-1</sup>.<sup>14</sup> In a similar titration experiment, chloroform exhibited a lower affinity toward **1**: the downfield shift of the N–H resonance was noticeable, yet insufficient to quantify the binding.<sup>14</sup> Variable-

(18) (a) Taft, R. W.; Gurka, D.; Joris, L.; Schleyer, P. v. R.; Rashys, J. W. *J. Am. Chem. Soc.* **1969**, *91*, 4801–4808. (b) Beeson, C.; Pham, N.; Shipps, G.; Dix, T. A. *J. Am. Chem. Soc.* **1993**, *115*, 6803–6812.

(19) Chapman, K. T.; Still, W. C. *J. Am. Chem. Soc.* **1989**, *111*, 3075–3077.

(20) Mecozzi, S.; Rebek, J., Jr. *Chem.-Eur. J.* **1998**, *4*, 1016–1022.

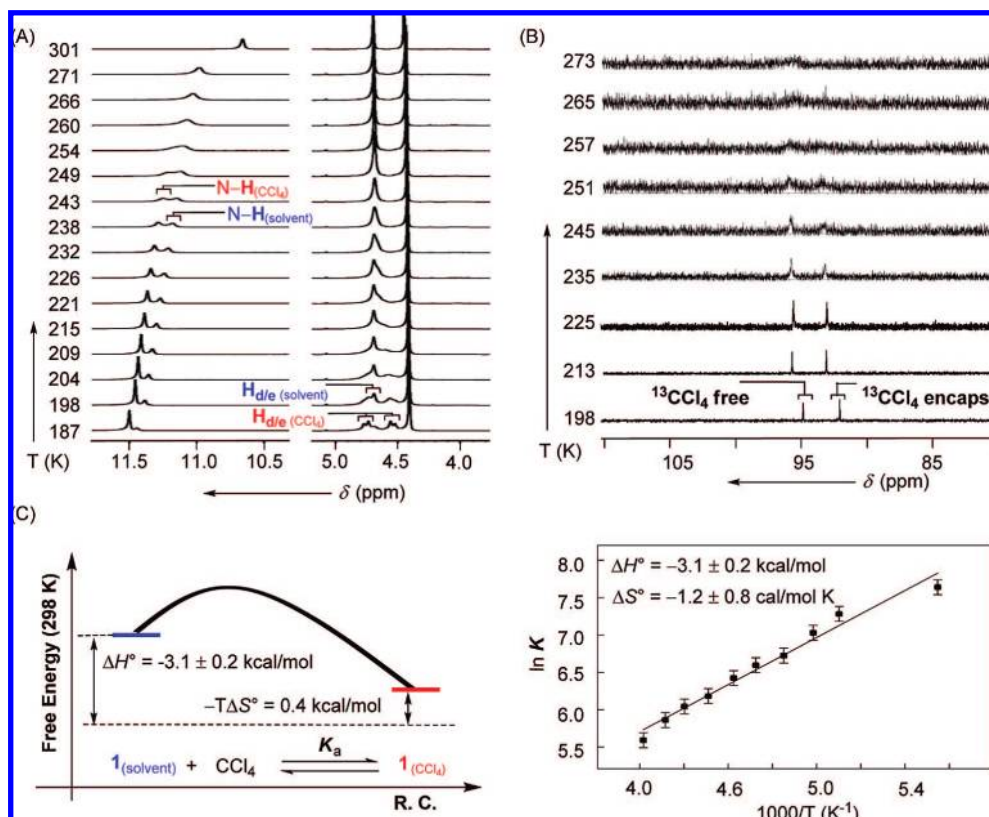


**Figure 5.** (A) Selected regions of variable-temperature (VT) <sup>1</sup>H NMR spectra (400 MHz, CD<sub>2</sub>Cl<sub>2</sub>) of a solution of **1** (2.4 mM) and CCl<sub>4</sub> (3.7 mM). (B) A selected region of VT <sup>13</sup>C NMR spectra (100 MHz) of a solution of **1** (13.1 mM) and <sup>13</sup>CCl<sub>4</sub> (19.6 mM). (C) van't Hoff plot and thermodynamic parameters for the **1**<sub>(solvent)</sub>/**1**<sub>(CCl<sub>4</sub>)</sub> equilibrium.

temperature (VT) <sup>1</sup>H NMR spectra (400 MHz) of a solution of **1** (2.4 mM, CD<sub>2</sub>Cl<sub>2</sub>), containing CCl<sub>4</sub> (3.7 mM), revealed decoalescence of signals at ca. 260 K (Figure 5A). Two sets of peaks developed, with the intensity ratio changing with temperature. Each group of signals has been assigned to a C<sub>3</sub> symmetrical basket: one occupied with the solvent (**1**<sub>(solvent)</sub>) and another with the added guest (**1**<sub>(CCl<sub>4</sub>)</sub>, Figure 5C). Indeed, when <sup>13</sup>CCl<sub>4</sub> was employed in the experiment (Figure 5B), the decoalescence in VT <sup>13</sup>C NMR spectra was observed at practically the same temperature (ca. 260 K). The resolved resonances at 96.0 and 93.0 ppm corresponded to free and encapsulated molecules of <sup>13</sup>CCl<sub>4</sub>, respectively. The integration of the N–H signals (Figure 5A), at each temperature, afforded association constants and thermodynamic parameters for the conversion of **1**<sub>(solvent)</sub> into **1**<sub>(CCl<sub>4</sub>)</sub> (Figure 5C). In essence, the incorporation of carbon tetrachloride into the basket is driven by enthalpy (ΔH° = -3.1 ± 0.2 kcal/mol). This, for the most part, can be viewed as a result of the favorable host/guest van der Waals contacts that CCl<sub>4</sub> affords on the account of its size (Table 1);<sup>20</sup> in fact, the apparent lower tenacity of smaller CH<sub>2</sub>Cl<sub>2</sub> for occupying **1** can be justified on the same basis.<sup>20</sup> Along with this guest occupation, there is concomitant change of the intramolecular HBs of the occupied host, as indicated by the observed lower-field <sup>1</sup>H NMR N–H signals of **1**<sub>(CCl<sub>4</sub>)</sub> versus **1**<sub>(solvent)</sub> (Figure 5A). The observed loss in entropy (ΔS° = -1.2 ± 0.8 eu) is negligible but, to a first approximation, congruent with the exchange of a solvent molecule, CD<sub>2</sub>Cl<sub>2</sub>, with a molecule of CCl<sub>4</sub>.

**Dynamic <sup>1</sup>H NMR Studies: The Kinetics of Molecular Folding and Translocation.** The basket **1**<sub>A</sub>/**1**<sub>B</sub> conformational equilibrium (Figure 3), manifested in the exchange of the H<sub>c/d</sub>

**Table 2.** Activation Parameters for the **1**<sub>A</sub>/**1**<sub>B</sub> Interconversion in CD<sub>2</sub>Cl<sub>2</sub>, CDCl<sub>3</sub>, and CD<sub>2</sub>Cl<sub>2</sub> Containing 50.0 mol equiv of CCl<sub>4</sub> (Eyring Plots Were Used To Generate the Data)<sup>14</sup>

solvent system	E <sub>r</sub> (30)	volume <sup>a</sup> (Å <sup>3</sup> )	ΔH <sup>‡</sup> (kcal/mol)	ΔS <sup>‡</sup> (cal/mol·K)
CD <sub>2</sub> Cl <sub>2</sub>	41	61	N/A	N/A
CDCl <sub>3</sub> <sup>b</sup>	35	75	11.5 ± 0.2	3.9 ± 0.1
CD <sub>2</sub> Cl <sub>2</sub> /CCl <sub>4</sub> <sup>c</sup>	41	89	10.4 ± 0.3	1.4 ± 0.1

<sup>a</sup> Calculated with Spartan Software. <sup>b</sup> T = 202–240 K. <sup>c</sup> T = 180–223 K.

spins (Figure 4), was subjected to a total band-shape analysis<sup>22</sup> to get the interconversion apparent first-order rate constants *k*<sub>1</sub>/*k*<sub>-1</sub> (Figure 4).<sup>23</sup> Subsequently, the activation parameters for the interconversion in (a) neat chloroform with CHCl<sub>3</sub>, and (b) CH<sub>2</sub>Cl<sub>2</sub> with CCl<sub>4</sub> as guests, were extracted from Eyring plots (Table 2).<sup>14</sup> Remarkably, the rates for the basket opening/closing (**1**<sub>A</sub>/**1**<sub>B</sub>) were nearly identical when bigger molecules CHCl<sub>3</sub> (75 Å<sup>3</sup>) or CCl<sub>4</sub> (89 Å<sup>3</sup>) occupied its cavity (221 Å<sup>3</sup>). The smaller CH<sub>2</sub>Cl<sub>2</sub> (61 Å<sup>3</sup>), however, did not “impose” on the basket’s conformational dynamics (Table 2), as the <sup>1</sup>H NMR spectroscopic results were invariant with temperature (T = 179–298

(21) (a) Wilcox, C. In *Frontiers in Supramolecular Organic Chemistry and Photochemistry*; Schneider, H.-J., Durr, H., Eds.; Wiley-VCH: Weinheim, 1991; pp 123–143. (b) Connors, K. A. *Binding Constants, The Measurement of Molecular Complex Stability*; Wiley-Interscience: New York, 1987; pp 24–28.

(22) (a) Kaplan, J. J.; Fraenkel, G. *NMR of Chemically Exchanging Systems*; Academic Press: New York, 1980. (b) Pons, M.; Millet, O. *Prog. Nucl. Magn. Reson. Spectrosc.* **2001**, *38*, 267–324. (c) Bain, A. D.; Rex, D. M.; Smith, R. N. *Magn. Reson. Chem.* **2001**, *39*, 122–126. (d) Bain, A. D. *Prog. Nucl. Magn. Reson. Spectrosc.* **2003**, *43*, 63–103.

(23) Reich, H. J. *WinDNMR: Dynamic NMR Spectra for Windows*; J. Chem. Ed.: Software, Series D, 1996.

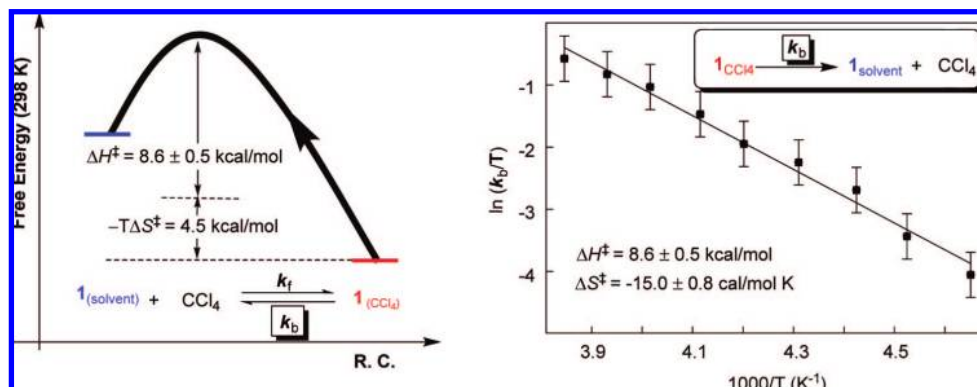


**Figure 6.** Eyring plot and the activation parameters for  $\text{CCl}_4$  departing  $\mathbf{1}_{(\text{CCl}_4)}$ , obtained from dynamic  $^1\text{H}$  NMR measurements in  $\text{CD}_2\text{Cl}_2$ .<sup>14</sup>

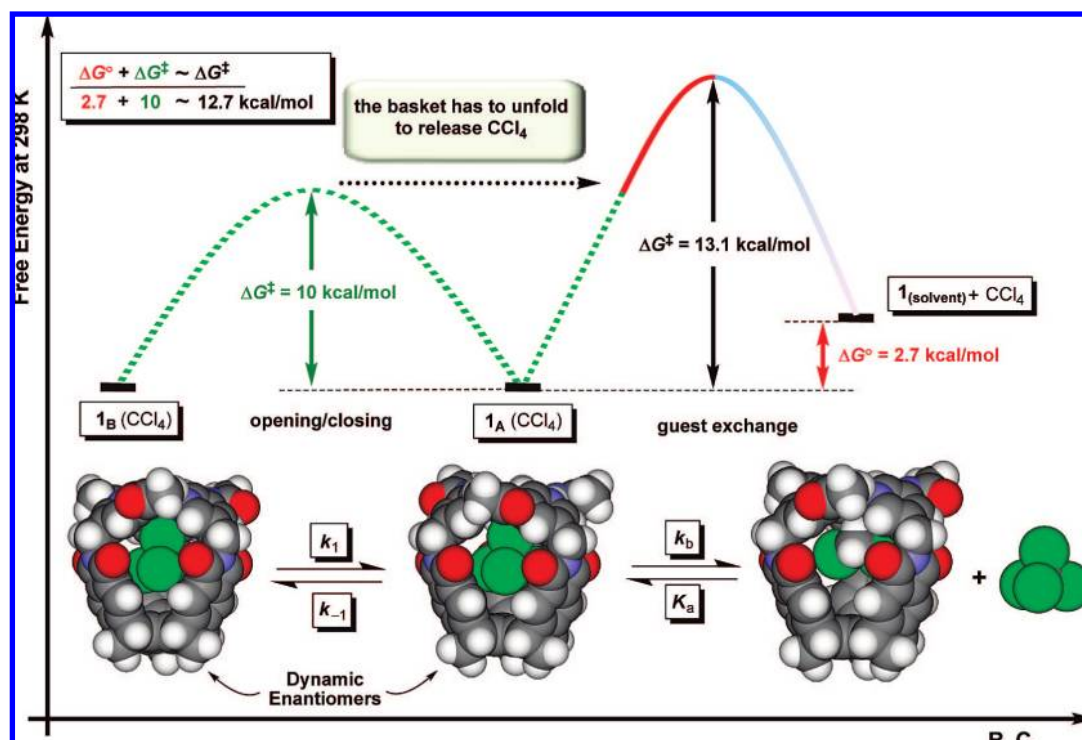


**Figure 7.** Energy diagram showing the partitioned standard ( $\Delta G^\circ$ ) and activation free energies ( $\Delta G^\ddagger$ ), at 298 K, for synchronized gated transfer of  $\text{CCl}_4$  in/out of molecular basket  $\mathbf{1}$ .

$\text{K}$ ).<sup>14</sup> As stated earlier, dichloromethane slippage<sup>24</sup> through the aperture of  $\mathbf{1}$  is energetically easier ( $\sim 7$  kcal/mol) and, evidently, is not correlated with the motion of the gates. In contrast, bigger guests ( $\text{CHCl}_3$  and  $\text{CCl}_4$ ) require more room to traffic into or out of the host  $\mathbf{1}$ , thus imposing on the  $\mathbf{1}_A/\mathbf{1}_B$  interconversion. Notably, this observation points to the correlation between the guest exchange and the gates' rotary motion and needs to be taken into account for elucidating the operational mechanism of the basket (see below).

We, furthermore, examined the apparent rate constant  $k_b$  for  $\text{CCl}_4$  departing  $\mathbf{1}_{(\text{CCl}_4)}$  at various temperatures (Figure 6), by simulating the line shapes of the two exchanging and unequally populated  $\text{N-H}$  spins<sup>21–23</sup> (Figure 5A): one corresponding to  $\mathbf{1}_{(\text{solvent})}$  and another to  $\mathbf{1}_{(\text{CCl}_4)}$  basket. From the Eyring plot (Figure 6), the activation enthalpy for  $\text{CCl}_4$  leaving the basket was found to be positive ( $\Delta H^\ddagger = 8.6 \pm 0.5$  kcal/mol), while the activation entropy was negative ( $\Delta S^\ddagger = -15.0 \pm 0.8$  eu).

**On the Encapsulation Mechanism.** With the acquired kinetic and thermodynamic information (Figure 7), the following question was posed: does the opening/closing of the basket, expressed via  $\mathbf{1}_A/\mathbf{1}_B$  interconversion, restrict (regulate) the kinetics of the egress/ingress of  $\text{CCl}_4$  molecules? Carbon tetrachloride is, in the context of  $\mathbf{1}$ , a sizable molecule. Its slippage through the aperture of the folded basket demands a high activation energy ( $> 14$  kcal/mol, PM3);<sup>14</sup> importantly, the calculation does not treat a more realistic guest swapping that requires a greater expansion of the host. Alternatively, the escape of the guest from the basket could be occurring by way of an opening that forms when the gates rotate about their axis ( $\mathbf{1}_A/\mathbf{1}_B$ , Figure 3). In fact, the revolving of gates takes a portion of the host's inner space occupied by  $\text{CCl}_4$ , presumably forcing the guest's departure to be correlated with motion of the host. Moreover, the rotary motion of the gates would not only be expected to guide the guest out but also to create two additional apertures for an incoming molecule to enter the host with almost no additional expense in energy. The conformational  $\mathbf{1}_A/\mathbf{1}_B$

(24) See, for instance: Raymo, F. M.; Houk, K. N.; Stoddart, J. F. *J. Am. Chem. Soc.* **1998**, *120*, 9318–9322.

interconversion bears 10.0 kcal/mol of the activation energy ( $\Delta G^\ddagger$ ) at 298 K (Table 2). Furthermore, a molecule of  $\text{CCl}_4$  is occupying the host with the complexation free energy ( $\Delta G^\circ$ ) of 2.7 kcal/mol at 298 K (Figure 5C). When the above two numerals are added ( $\Delta G^\ddagger + \Delta G^\circ$ ), an approximate activation energy for the exit of  $\text{CCl}_4$  is expected on the order of 12.7 kcal/mol (Figure 7).<sup>7</sup> Remarkably, the experimental activation free energy ( $\Delta G^\ddagger$ ) for  $\text{CCl}_4$  departing the basket was found to be 13.1 kcal/mol at 298 K (Figure 6). In fact, when the kinetics and thermodynamics for the entrapment of bigger  $(\text{CH}_3)_3\text{CBr}$  ( $107 \text{ \AA}^3$ ) were examined, the energetics appeared to be additive as well (Figures S19–S24,  $\Delta G^\ddagger_{\text{(experimental)}} = 11.8 \text{ kcal/mol}$  vs  $\Delta G^\ddagger_{\text{(calculated)}} = 12.4 \text{ kcal/mol}$ ).<sup>14</sup> The evaluated free energies ( $\Delta G^\ddagger_{\text{(experimental)}}$  and  $\Delta G^\ddagger_{\text{(calculated)}}$ ) indeed alter with temperature, but the proposed additive relationship<sup>25</sup> holds reasonably well at the investigated 200–300 K. The apparent absence of the additivity for the corresponding enthalpies and entropies, however, is indicative of the enthalpy/entropy compensation.<sup>26</sup> Likewise, the uncertainty in the experimental enthalpy and entropy<sup>27,28</sup> perhaps contributes to the apparent discrepancy. One can additionally anticipate that the exchange of  $\text{CCl}_4/(\text{CH}_3)_3\text{CBr}$  (or any other guest) may be dominated by the energetics being additive, provided that the guest occupies a sufficiently small portion of the host's cavity. Rebek and co-workers<sup>20</sup> have suggested that 55% of the inner space is an upper bound. We compute that  $\text{CCl}_4$  occupies 40% while  $(\text{CH}_3)_3\text{CBr}$  48% of the host inner space, thus leading to the observed additive energetics.<sup>29</sup> A correspondence between the estimated and the experimental activation barriers (Figure 7) suggests a synchronized gating mechanism, operating in the action of **1**! The gates must revolve, each about its axis, to form a corridor for molecules to exchange in a way akin to the operation of a butterfly valve in regulating the flow of liquids. Importantly, the rotation of the gates may sweep a part of the basket's inner space, occupied by a guest, to impose on the exchange process.<sup>30</sup> The discovery

indicates a new mechanism<sup>31</sup> for regulating the encapsulation's kinetic stability and adds to the scope of the french/sliding door formalism<sup>6</sup> and other known pathways<sup>31</sup> for the exchange of guests to and from synthetic hosts.

## Conclusions

Maneuvering the kinetic stability of a host–guest complex necessitates an ability to synchronize multiple dynamic structural elements within the host. This study exemplifies the design of a molecular basket capable of regulating the trafficking of guests using a set of functionalized aromatics – gates. The gates assemble via intramolecular hydrogen bonding to enfold space. The rotary motion of the gates, each about its longitudinal axis, forms a dynamic corridor to impose on guests to exchange to and from the interior. Such a new mechanism for the dynamic regulation of molecular encapsulation creates a unique opportunity to explore the interdependence of kinetic stability and chemical reactivity, as well as the controlled translocation of molecules in artificial environments.

**Acknowledgment.** We thank Professor Gideon Fraenkel of the Ohio State University for useful suggestions. This work was financially supported with funds obtained from the Ohio State University, and the National Science Foundation under CHE-0716355. Generous computational resources were provided by the Ohio Supercomputer Center.

**Supporting Information Available:** Additional experimental and computational results. This material is available free of charge via the Internet at <http://pubs.acs.org>.

JA8041977

- (25) Dill, K. A. *J. Biol. Chem.* **1997**, *272*, 701–704.  
(26) Liu, L.; Guo, Q.-X. *Chem. Rev.* **2001**, *101*, 673–695.  
(27) Exner, O. *Nature* **1970**, *227*, 366–367.  
(28) (a) Alper, J. S.; Gelb, R. I. *J. Phys. Org. Chem.* **1993**, *6*, 273–280. (b) Gelb, R. I.; Alper, J. S. *J. Phys. Org. Chem.* **1995**, *8*, 825–832.  
(29) The hypothesis is currently under investigation with differently sized guests, and the results will be reported in due course.  
(30) (a) Jiang, X.; Bollinger, J. C.; Lee, D. *J. Am. Chem. Soc.* **2006**, *128*, 11732–11733. (b) Riddle, J. A.; Jiang, X.; Huffman, J.; Lee, D. *Angew. Chem., Int. Ed.* **2007**, *46*, 7019–7022. (c) Riddle, J. A.; Jiang, X.; Lee, D. *Analyst* **2008**, *133*, 417–422.

- (31) Other scenarios acting in the exchange of guests cannot be ignored; for example, another mechanistic possibility is the rotation of one pyridyl arm versus the motion of all three arms. Each postulated mechanism may be a function of the guest characteristics and will certainly benefit from additional experimental scrutiny. In this study, however, IR spectroscopy showed that the N–H hydrogen-bonding pattern was dominated by intramolecular HBs, and little evidence was seen for a free pyridyl arm. Calculations are in support of this observation. Moreover, preliminary results of our molecular dynamics (MD) and steered molecular dynamics simulations with the Amber suite of programs indicate the rupture of all three N–H...N hydrogen bonds occurs in the removal of  $\text{CCl}_4$  from the interior of **1**. Experimental and computational studies are in progress to reveal mechanistic details. See also: Pluth, M. D.; Raymond, K. N. *Chem. Soc. Rev.* **2007**, *36*, 161–171.